
This is an electronic reprint of the original article.
This reprint may differ from the original in pagination and typographic detail.

Alibakhshi, Sara; Hovi, Arne; Rautiainen, Miina

Temporal dynamics of albedo and climate in the sparse forests of Zagros

Published in:
Science of the Total Environment

DOI:
[10.1016/j.scitotenv.2019.01.253](https://doi.org/10.1016/j.scitotenv.2019.01.253)

Published: 01/05/2019

Document Version
Publisher's PDF, also known as Version of record

Published under the following license:
CC BY

Please cite the original version:
Alibakhshi, S., Hovi, A., & Rautiainen, M. (2019). Temporal dynamics of albedo and climate in the sparse forests of Zagros. *Science of the Total Environment*, 663, 596-609. <https://doi.org/10.1016/j.scitotenv.2019.01.253>

This material is protected by copyright and other intellectual property rights, and duplication or sale of all or part of any of the repository collections is not permitted, except that material may be duplicated by you for your research use or educational purposes in electronic or print form. You must obtain permission for any other use. Electronic or print copies may not be offered, whether for sale or otherwise to anyone who is not an authorised user.



Temporal dynamics of albedo and climate in the sparse forests of Zagros

Sara Alibakhshi ^{a,*}, Arne Hovi ^a, Miina Rautiainen ^{a,b}

^a Department of Built Environment, School of Engineering, Aalto University, P.O. Box 14100, 00076 Aalto, Finland

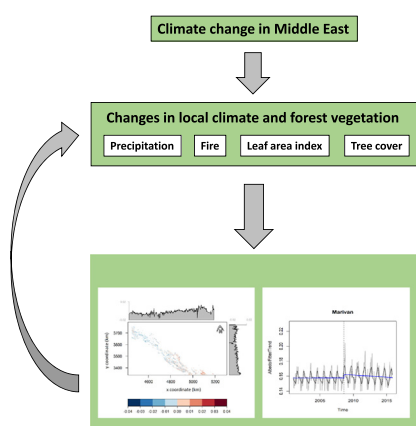
^b Department of Electronics and Nanoengineering, School of Electrical Engineering, Aalto University, P.O. Box 15500, 00076 Aalto, Finland



HIGHLIGHTS

- The Middle East is suffering from significant climate change and deforestation.
- Analyses of albedo dynamics in the largest forest area in the Middle East (Zagros)
- First report of links between climate, burn severity, LAI and albedo in Zagros
- Albedo dynamics are strongly linked with the number of fire events and LAI.

GRAPHICAL ABSTRACT



ARTICLE INFO

Article history:

Received 23 August 2018

Received in revised form 22 December 2018

Accepted 19 January 2019

Available online 23 January 2019

Editor: Ralf Ludwig

Keywords:

Albedo

LAI

Fire and drought

Climate change

Zagros forest

Middle East

ABSTRACT

Land surface albedo is an important parameter affecting the climate locally and globally. A synthesis of current studies urgently calls for a better understanding of the impact of climate change on the surface albedo. The Middle East is expected to experience major climatic changes during the coming decades and has already undergone major losses in its vegetation cover. This study explores how climate change related disturbances, such as severe drought and fire events, influence albedo trends in the largest remaining forest area of the Middle East, the Zagros Mountains. We analyzed time series of albedo, Leaf Area Index (LAI), burn severity (dNBR), and the number of fire events all obtained from MODIS satellite images between 2000 and 2016, together with climatic data from 1950 to 2016. The Zagros area is continuously suffering from low precipitation, high temperatures, and evermore-frequent wildfire events. Our large-scale analysis revealed that albedo is linked to precipitation, number of fire events, dNBR, and LAI with the average correlation coefficients of -0.26 , -0.50 , 0.17 , and -0.72 , respectively. Using four study sites located in different parts of the Zagros area, we showed disturbances influence albedo differently. Drought condition resulted in a marginal increasing trend in albedo, whereas fire events resulted in a decreasing trend. This article is the first report linking climate change with albedo in Iran.

© 2019 The Authors. Published by Elsevier B.V. This is an open access article under the CC BY license (<http://creativecommons.org/licenses/by/4.0/>).

1. Introduction

Land surface albedo, the fraction of incoming solar radiant flux hemispherically reflected from the Earth surface, has been identified as a critical variable determining the planet energy absorption and in turn local and global climate variability (Bright et al., 2015). Due to its

* Corresponding author.

E-mail address: sara.alibakhshi@aalto.fi (S. Alibakhshi).

critical role in the energy balance, the Global Climate Observing System lists albedo as an essential climate variable (GCOS, 2006). Nevertheless, confidence in albedo-related radiative forcing estimation remains relatively weak (Pitman et al., 2009).

The Earth surface characteristics can determine the amount of energy absorptance of an ecosystem (Bright et al., 2017). Changes in the Earth surface including removal of canopy cover under influence of the disturbances, and/or establishment of grasses and shrubs and trees can substantially change surface albedo (e.g., Abera et al., 2019). When disturbances occur, the albedo (reflectivity) of an ecosystem can either increase or decrease if the ecosystem becomes lighter (e.g., by more exposing bare soil after plant removal), or darker (e.g., remaining black charcoal after the fire) (Gatebe et al., 2014; Govaerts and Lattanzio, 2007). The increases in the surface albedo can then lead to a negative radiative forcing, i.e. increase in outgoing energy flux from the Earth system, and therefore cooling effects. The opposite scenario is true for decreases in the surface albedo (IPCC, 2018).

Driving factors of forest albedo are, for example, forest structure, biomass and species composition (Lukeš et al., 2013), which can significantly change when disturbances occur (Running, 2008). Disturbance rates in forest ecosystems have increased to an alarming level (Hansen et al., 2013). According to FAO, natural forest areas have declined from 4128 Mha to 3999 Mha between the years 1990 and 2015 (Keenan et al., 2015). Globally, wildfire events affect 350 Mha of forests annually (FAO, 2003), and burned areas have increased by ~37% during the past two decades (i.e., from 1997 to 2016) (Van der Werf et al., 2017). Such a high rate of changes in forest ecosystems can highlight the importance of albedo studies, as albedo is a critical variable of explaining future Earth climate.

Although various forest disturbances have substantially increased globally, their relationships with albedo and consequences to climate are still poorly known (Bonan, 2008; Bright et al., 2015; Kurz et al., 2008). Even in recent studies, the role of disturbances in explaining albedo and net climate forcing has been ignored (Alkama and Cescatti, 2016) because the link between different types of ecosystem disturbances and albedo have not yet been established. One reason is the complexity of determining such relationships.

To investigate the link between albedo and disturbances, many studies have been conducted. Some studies have shown that fire events resulted in albedo decrease in forests (Dintwe et al., 2017), while in some other studies, albedo tends to increase after the fire events (O'Halloran et al., 2012). In particular, multiple studies used albedo time series of MODIS products and manifested that loss of overstory through drought condition can lead to greater exposure of snow-covered surfaces or bare soil and in turn, albedo increases (Liu et al., 2005; Lyons et al., 2008). In contrast, it has been shown that if a fire happened, black carbon on soils and the boles of dead trees can reduce albedo by darkening the background (Chambers and Chapin, 2002). Moreover, establishment and growth of herbaceous plants, shrubs, and deciduous trees can cause rapid increases in summer albedo after a disturbance (Lyons et al., 2008). The magnitude of albedo changes can vary due to pre-disturbance vegetation structure, soil properties, vegetation regrowth, and recovery rates, and time and duration of disturbances (Gitas et al., 2012; Schwaiger and Bird, 2010). Hence, it is unclear to what extent disturbances will influence albedo and eventually net climate forcing.

To address this knowledge gap, we need empirical studies to link time series of albedo and vegetation, i.e., Leaf Area Index (LAI) and tree cover data, with actual disturbance events in forest ecosystems. Such studies will help to understand how ecosystems respond to ecological catastrophes, such as severe drought or fire event, and may improve climate change projections.

This paper focuses on the Middle East, which along with Eastern Mediterranean is one of the 'hot spots' likely to experience major climate change effects in the twenty-first century (Giorgi and Lionello, 2008; Lelieveld et al., 2012). Several studies have illustrated a consistent climate change over the region in the last decades (Kaniewski et al., 2012; Lelieveld et al., 2016). ENSO may be the reason for the

unexpectedly intense climatic anomaly in 2007–2008 in the Middle East (Barlow et al., 2016). This phenomenon had negative consequences in western Iran in 2007–2009, as the severest drought from 1960 to 2009 (Voss et al., 2013; Hosseinzadeh Talaei et al., 2014). In addition, ENSO resulted in significant hydrological drought in Iran (i.e., increases in snowmelt, decrease in precipitation, soil moisture and water areas in the ground waters, streams, lakes, and reservoirs) (Voss et al., 2013). Besides making the lives of humans very difficult, these extreme climatic events already evidently increase the risks of various forest disturbances in the few remaining forests and woodland areas (Barlow et al., 2016).

In the Middle East, Iran is among the worst drought-affected areas (Kaniewski et al., 2012). Based on data provided by the Global Forest Watch, Iran has experienced a dramatic 58% increase in forest wildfire events from 2012 to 2016 (GFW, 2014). Currently, Iran and Turkey are the most forested countries in the Middle East (Ma, 2008). One of the largest forest and woodland areas in this region is located in the Zagros Mountains, which expands a length of 1600 km (from north to south) and around 240 km (from east to west) through Iran, Turkey, and Iraq (Kolahi-Azar and Golriz, 2018). The Zagros ecosystem has a high biodiversity richness, but the International Union for Conservation of Nature and Natural Resources (IUCN) Red List identified many of the area's species as vulnerable and endangered (IUCN, 2001) because the area is faced with wide deforestation associated with urban population growth and climate change (Henareh Khalyani and Mayer, 2013; Henareh Khalyani et al., 2013). Recently, this sparse, oak-dominated forest area has been affected by severe drought (Arsalani et al., 2015; Azizi et al., 2013), fire (Heydari et al., 2016), and fungal pathogens attacks, leading to a dramatic dieback of the oak forests (Mirabolfathy et al., 2011). The high deforestation rate has placed Iran among the top 10 Asian and Pacific countries with destroyed and degraded forests (Saleh Arekhi, 2011). The magnitude of the environmental changes in the Zagros mountains has been considerable, and the Food and Agriculture Organization of the United Nations (FAO) has initiated efforts to protect the area.

The main objective of this paper is to explore how climate change related disturbances, including severe drought, the number of fire events, and burn severity can influence albedo. For this purpose, we hypothesized that major vegetation changes in both understory and overstory (as quantified by remotely sensed LAI and tree cover) can be linked with the dynamics of albedo in the entire Zagros area and at smaller study sites during a study period ranging from 2000 to 2016. In addition, we hypothesized that climate change related disturbances such as the number of fire events and burn severity will significantly reduce the albedo while drought conditions can result in an opposite response. To test this hypothesis, we analyzed long-term changes in climate variables in the Middle East for years 1950–2016 as background information. Further, we investigated the time series of albedo, LAI, the number of fire events, and burn severity obtained from Moderate Resolution Imaging Spectroradiometer (MODIS) satellite images, as well as precipitation rate obtained from Community Earth System Model version1–Biogeochemistry (CESM1-BGC) and National Centers for Environmental Prediction/National Center for Atmospheric Research (NCEP/NCAR) for the years 2000–2016. To determine the potential links between disturbances (droughts and fire events) and temporal trends of albedo, we used two methods including Pearson correlation test and the breaks for an additive seasonal trend (BFAST). We performed analyses at two scales: first for the largest forest area in the Middle East, the Zagros Mountains, for an area covering 384,000 km², and secondly, for four study sites, located in different parts of the Zagros area. We also estimated the tree cover as an independent source of data to determine the contribution of overstory to the temporal dynamics of albedo. Despite the importance of albedo and its physical relationships with future climate, the majority of studies have been conducted in the boreal zone and only a few studies in the other biomes. This implies a geographic gap that would be a source of bias for our understanding, which has been addressed in this study. This paper is the first report linking albedo and climate change in forest areas in Iran.

2. Materials and methods

In this section, we first describe the study sites (Section 2.1–2.2) and then provide information about the selection of the datasets and their preprocessing steps (Section 2.3). Finally, we describe how time series of satellite images have been processed and used for spatio-temporal analyses (Section 2.4).

2.1. Study area: northern and southern Zagros

The Zagros area extends to an area of 1600 km in length (north to south) and around 240 km in width (east to west) in western and southwestern Iran, northern Iraq, and southeastern Turkey (Kolahi-Azar and Golriz, 2018) (Fig. 1). According to the national land use map of Iran, the Zagros area in Iran is covered by sparse forest with a total area of 102,995 km² (Landuse Map, 2000). The Zagros forests are dominated by *Quercus* species such as *Quercus persica*, *Quercus infectoria*, and *Quercus libani*. The majority of tree species and understory species are deciduous in this area (Fathizadeh et al., 2017; Olfat and Pourtahmasi, 2010). The area is typically characterized by a semi-humid climate with cold winters and total annual precipitation exceeding 800 mm (Bazyar et al., 2013).

The portion of the Zagros area in Iran can be divided into two parts (the northern Zagros and the southern Zagros) based on climate conditions (Fig. 1) (Henareh Khalyani and Mayer, 2013). The northern Zagros covers an area of approximately 42,064 km², and the southern Zagros covers an area of 60,931 km². The northern Zagros is wetter and cooler than the southern Zagros, especially in winter time (December through February). The mean monthly temperature (in years 2000–2016) in the northern Zagros, ranges from 0 °C to 30 °C, but in the southern Zagros, it ranges from 10 °C to 40 °C, according to CESM1-BGC and NCEP/NCAR datasets (Hurrell et al., 2013; Kalnay et al., 1996).

2.2. Study sites

In this paper, four sites were chosen within the Zagros area for a detailed study based on the coordinates provided by fire stations' reports, and the experts working in Environmental and Forestry Organization, University of Tehran, Ilam, and Malayer in Iran. We selected these study sites because they represent different types of disturbance patterns related to forest fires and drought (extended periods of relatively low precipitation), both leading to defoliation of trees. Two sites (Marivan, Ilam) are located in the northern Zagros, and the other two (Ize, Dashte baram) in the southern Zagros area (Fig. 1, Table 1, Appendix A1).

The tree layers in Marivan and Ilam are dominated by *Q. brantii* and/or *Q. boissieri*, whereas Ize and Dashte baram are the exclusive domain of *Q. persica* (Henareh Khalyani and Mayer, 2013). Beneath the tree layer, there is an understory layer of herbs and small shrubs (e.g. *Astragalus* spp., *Salvia* spp.) in the northern Zagros (Heshmati, 2007). In the southern Zagros, on the other hand, the understory layer is dominated by hawthorns (*Crataegus* sp.) and small tree species such as almonds (*Prunus amygdalus*), nettle trees (*Celtis* sp) and pears (*Pyrus* spp.) (Heshmati, 2007). The dominant soil is “rock outcrops or entisols” in Marivan, Ilam, and Ize, and “rock outcrops or inceptisols in Dashte baram (STP, 2015).

All four study sites are relatively homogeneous and suffer from fungus attacks by *Biscogniauxia mediterranea*, causing charcoal disease, and beetle attacks by *Agrilus hastulifer* (Taghimollaei and Karamshahi, 2017; Mirabolfathy, 2013; Safaei et al., 2016). Drought is a major disturbance of Marivan and Dashte baram sites. According to the local reports and Global Forest Watch, fire is the main disturbance of forests in Ilam and Ize (GFW, 2014).

2.3. Datasets

2.3.1. Climate datasets

To visualize climate change over the Middle East as background information, monthly data on land surface temperature, precipitation rate, and

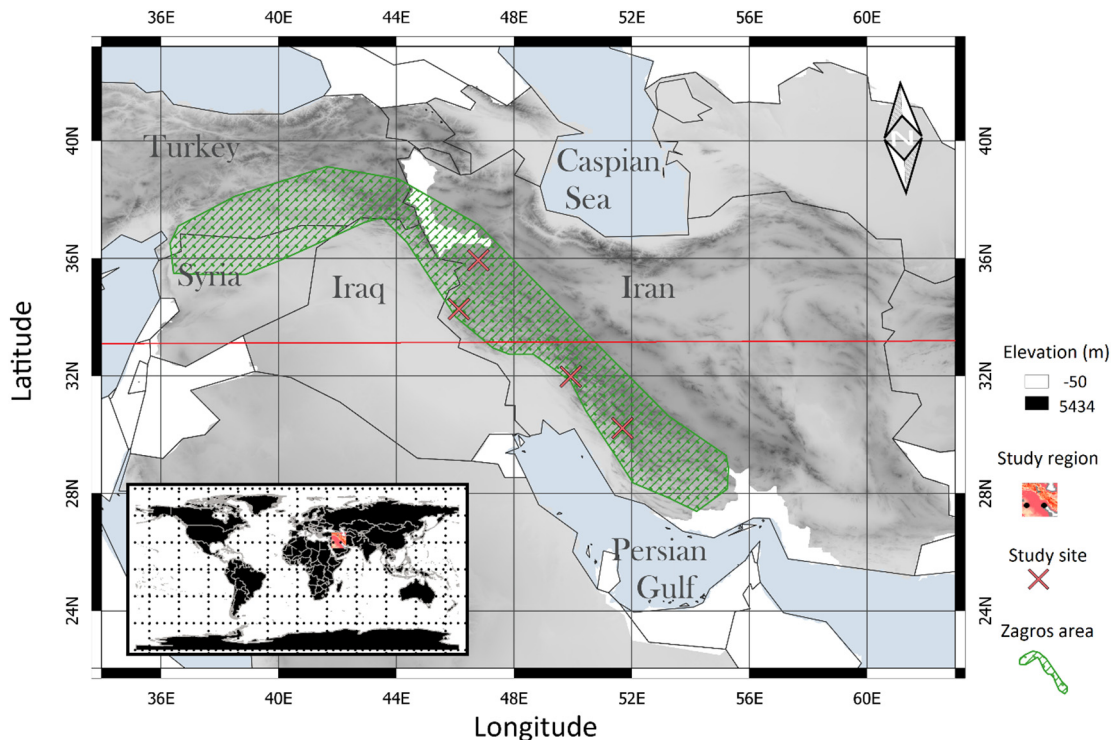


Fig. 1. The study area. The green area refers to Zagros forests. The topography of the area is shown as an elevation map in the background. The horizontal red line (~33°N) shows the division of Zagros into the northern and southern parts (Henareh Khalyani et al., 2013). The green polygons approximately refer to the area of Zagros (Doubek, 2013). The multiplication signs refer to Marivan, Ilam, Dashte baram and Ize study sites from northern to southern area, respectively.

Table 1

Summary of study sites. All study sites also suffered from fungus and beetle attacks.

Site	Region	Disturbance	Coordinate ^a (latitude/longitude)	Number of MODIS pixels	Percentage of missing data ^b [%]	Range of elevation (minimum–maximum) [m]
Marivan	Northern Zagros	Severe drought	35°39'11"N 46°24'55"E	34	18	1702–1726
Ilam	Northern Zagros	Forest fires	33°38'6"N 46°34'50"E	42	14	1004–1040
Ize	Southern Zagros	Forest fires	31°57'2"N 49°58'5"E	54	10	1515–2506
Dashte baram	Southern Zagros	Severe drought	29°35'28"N 51°48'47"E	88	7	1197–1763

^a The coordinate corresponds to the approximate center point of the study site (Appendix 1).^b The percentage of the missing values over each time series between 2000 and 2016; the information about the quality of the albedo values were used to remove the low quality pixels that were considered as missing values (Section 2.3.3)

evapotranspiration were collected in a $0.5^\circ \times 0.5^\circ$ grid from Iran, Iraq and Turkey extending from 35° to 60° E, and from 24° to 42° N. The data obtained from the FetchClimate Explorer site (©2014 Microsoft Corporation) for years 1950–2016 that are available in R software as the 'RfC' package (Grechka et al., 2016; Smith et al., 2014). The idea behind the FetchClimate is to obtain long-term climate data from multiple sources of the climate data for the examined sites and to select the most reliable datasets among available datasets for the given area. In this study, FetchClimate used CESM1-BGC, along with NCEP/NCAR for observations of the temperature and precipitation and, FetchClimate data for observations of evapotranspiration (Hurrell et al., 2013; Kalnay et al., 1996). CESM1-BGC and NCEP/NCAR are publicly available tools to investigate Earth system interactions changes globally (Hurrell et al., 2013). The used climate data in this study have a coarse spatial resolution. However, due to the high temporal resolution of these datasets (i.e., monthly), they help to understand the general pattern of climate change in the Middle East, where long-term high spatial resolution data are rarely available.

2.3.2. Number of fire events and burn severity datasets

We obtained binary information about fire occurrence from the daily Fire Information for Resource Management System (FIRMS) dataset of MCD14DL satellite products in the Zagros area for years 2000–2016 (FIRMS, 2018). In the FIRMS dataset, each pixel on a given day has been classified as “fire” or “non-fire” depending on whether or not a fire was detected in the pixel on that particular day. The product uses the standard MODIS collection 6 of Fire and Thermal Anomalies product at 1-km resolution (MOD14/MYD14), along with Visible Infrared Imaging Radiometer Suite (VIIRS) active fire product at 375-m resolution that is the latest added product to the FIRMS (i.e., since 2011). The fire-detection algorithm of this product relies on the estimation of temperatures using thermal infrared wavelengths that can discriminate active fires at different resolutions (i.e., 100 m^2 to 1 km^2) (Giglio et al., 2003, 2016). The confidence of the product has been estimated by additional comparison analyses of near-coincident Aqua/MODIS, TET-1 (German Aerospace Center) active fire data, and other higher resolution products such as VIIRS (Giglio et al., 2003, 2016). We estimated the number of fire events by counting the number of fire pixels detected in a study area over a time period. We filtered out the FIRMS observations with confidence <75% to avoid false alarming.

We used bands 2 and 7 (near infrared, NIR, and shortwave infrared, SWIR, respectively) of the MOD09A1-version 6 MODIS product, at 500 m resolution for every 8 days between 2000 and 2016 to quantify a normalized burn ratio (NBR), and a difference NBR (dNBR). For each pixel, a value was selected for each 8-day composite considering the absence of clouds or cloud shadow, and aerosol loading.

These indices were quantified only for pixels with fire events (as identified by the FIRMS MODIS product) to characterize the degree of burn severity (Key and Benson, 2006). The NBR index (Eq. (1)) was calculated by taking the difference between near and shortwave infrared reflectance bands, normalized by the sum of these bands:

$$\text{NBR} = \frac{\text{NIR} - \text{SWIR}}{\text{NIR} + \text{SWIR}} \quad (1)$$

We applied the bi-temporal image differencing on pre- and post-fire NBR data (one year) to quantify dNBR (Key and Benson, 2006):

$$\text{dNBR} = \text{NBR}_{\text{pre-fire}} - \text{NBR}_{\text{post-fire}} \quad (2)$$

We defined the pre- and post-fire data needed in the computations in the following way. First, we considered potential phenological effects. It has been shown that the seasonal timing highly impacts the burn severity (dNBR) measures, and specifically for Mediterranean-type forests, the summer period has been recommended as preferential for fire/burn severity assessments (Veraverbeke et al., 2010b). Thus, we decided to use only data from summer periods (i.e., the months of June, July and August) to compute the yearly post- and pre-fire NBR values at each pixel. NBR data from all other months were discarded. We aggregated all NBR data from the summer before the fire event occurred to compute the pre-fire values, and similarly, all NBR data from the summer after the fire event had occurred to compute the post-fire values. Following (Lanorte et al., 2013), we considered the levels of burn severity as low severity if it was between +0.1 to +0.27, moderate severity if it was between +0.27 to +0.66, and high severity if it was greater than +0.66.

2.3.3. Albedo

We explored the time series of black-sky shortwave albedo at local solar noon from MODIS satellite images (MCD43A3 Collection 5 product) from 2000 to 2016. The MODIS BRDF/albedo algorithm is based on a semi-empirical kernel-driven bi-directional reflectance model, which is applied to multi-date MODIS satellite images, and it provides global albedo products of the land surface in 500 m spatial resolution every eight days. MCD43A2 contains incremental quality values associated with the retrieval performance at each pixel. The root mean square error of the MODIS Collection 5 shortwave albedo has been reported as 0.05 (Román et al., 2009). The albedo product does not yet include a topographic correction. Topographic effects could be the source of major error in mountainous areas such as the Zagros area. Therefore, using a Digital Elevation Model (DEM) with 90 m resolution (Jarvis et al., 2008), we estimated a slope map (Fleming and Hoffer, 1979). Then, we filtered out the MODIS pixels, which had a slope of $>5^\circ$. This led to total removal of <12% of MODIS pixels in the entire Zagros area. The four study sites, on the other hand, were located on flat terrain, and thus, no MODIS pixels were removed from the analyses covering these sites. For the albedo product, we used only the best quality retrieval results with snow-free pixels.

2.3.4. Leaf Area Index (LAI)

Vegetation greenness can be characterized by LAI that can be retrieved from optical satellite data. We used MODIS LAI (MCD15A2 Collection 5, 8-day composite, 500 m \times 500 m spatial resolution) product as ancillary data. MODIS LAI is estimated from atmospherically corrected bi-directional reflectance factors in the red and NIR spectral bands of MODIS data using a radiative transfer model designed for vegetation (Knyazikhin et al., 1998). For the LAI product, we used only best quality retrieval results with snow-free pixels based on the main algorithm retrievals (both with and without saturation).

2.3.5. Tree cover estimation

Satellite LAI products may correspond to the total LAI of a pixel, meaning both understory and overstory vegetation (e.g. (Majasalmi et al., 2015)). However, having high spatial resolution information on only the tree layer is needed to distinguish post-disturbance changes occurring in the tree layer from changes occurring in the understory layer. To estimate tree cover, we used high-resolution images available in Google Earth (Table A1) by randomly laying 400 points onto the satellite image of each study site, i.e., 1600 points in total, using R software (R Core Team, 2018). After classifying visually each point as a “tree” or “no tree” in the satellite images, we finally calculated the percentage of tree cover in the study site as the ratio of “tree” points to the number of total points.

A sufficient number of points for the relatively small and homogeneous study sites was 400 following standard error (SE) formula (Lindgren, 1966, as cited by Nowak and Greenfield, 2010):

$$p = \frac{n}{N} \quad (3)$$

$$SE = \sqrt{\frac{p * (1-p)}{N}} \quad (4)$$

where N is a total number of sampled points and n is a total number of points classified as a tree. In the formula, p is the ratio of number of trees to total number of sample points.

The tree cover was estimated twice for each study site: before and after the breakpoint in albedo time series (see Section 2.4.1 for determination of breakpoints from time series data) in order to explore if and how much tree cover in each site had changed. We selected the image closest to the breakpoint based on the availability of high-resolution satellite data through Google Earth.

2.4. Analyses of climate variables, fire events, LAI and albedo

To map the climate change from 1950 to 2016, we first applied a moving average with a window size of one-year in each pixel of the climate variables to avoid the seasonal effects and estimate the general

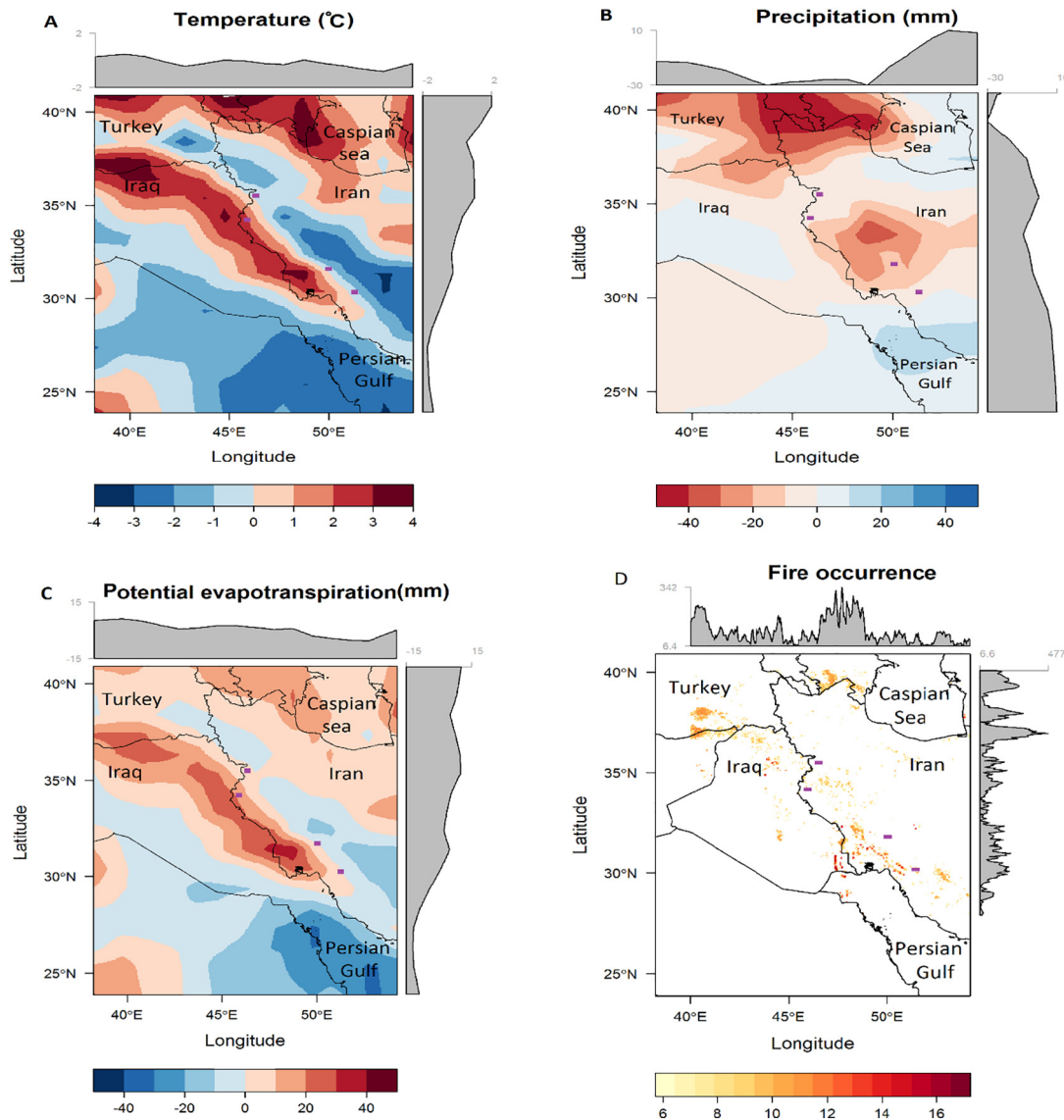


Fig. 2. A–C: The magnitude of change in climate variables between the periods, 1950–1955 and 2011–2016 in the Middle East region; the gray shades, on the top and the right of the graphs, refer to the mean magnitude of change in the values of the graphs over the longitudes and latitudes, respectively. A: Monthly mean temperature (°C). B: Monthly mean precipitation (mm). C: Monthly mean potential evapotranspiration (mm). D: The sum of number of fire events in the Middle East in the years 2000–2016; the gray shades, on the top and the right of the graph (D), refer to the total number of fire events from 2000 to 2016 over longitudes and latitudes, respectively. The areas located at the latitudes >33°N are in the northern Zagros in Iran. The purple rectangles refer to Marivan, Ilam, Dasht-e Barmam and Ize from north to south, respectively. (For interpretation of the references to colour in this figure legend, the reader is referred to the web version of this article.)

trend in a year. Then, to obtain an overview of how the climate has changed through the time, we estimated the magnitude of change by comparing the recent climate changes in the time series with the period that we considered as a reference. The reference time was selected before 1960 because the previous studies showed that the significant drought condition in the Middle East started from 1960 (Lelieveld et al., 2012). Thus, we calculated the difference between the mean of the last five years (from 2011 to 2016) and the mean of first five years (from 1950 to 1955) in the smoothed time series of the climate variables for each pixel. We selected a five-year window to avoid possible errors caused by extreme events. The results were shown as a map, where each pixel represents the magnitude of change obtained by comparison of 1950 to 1955 and 2011 to 2016 (Fig. 2). Furthermore, we mapped the frequency of fire events by estimating the sum of the number of fire occurrences at each pixel and mean of burn severity (Section 2.3.2) in the Middle East from 2000 to 2016.

We also mapped the albedo and LAI change in the Zagros forest between 2000 and 2016 to visualize how these variables changed over time using R software (Naimi, 2017; Hijmans, 2017; Lamigueiro and Hijmans, 2018). First, we filtered out the non-forest areas using a land use mask. The mask was obtained from the national Landsat-based land cover map of Iran produced by the Iranian Agricultural Organization (Landuse Map, 2000). Pixels with low albedo or LAI retrieval quality and/or snow cover were also filtered out (see Section 2.3.3). Next, we smoothed the time series data at each pixel using a moving average with a window size of one year. Finally, using the smoothed time-series, we estimated the pixel-wise magnitude of change of albedo and LAI by calculating the difference between the mean values of the variable obtained from the first two years and the last two years of the time period. We selected a two-year time window to ensure that a sufficient number of high-quality retrievals are included in the analyses. This also decreased the potential influence of extreme short-term events such as precipitation anomaly.

To explore the temporal dynamics of climate variables, fire event counts, albedo and LAI, we delineated pixels within northern and southern Zagros areas as well as in the four study sites. Time series of climate variables, albedo and LAI were smoothed using a moving average filter with a window size of one-year. The smoothed time series of precipitation, fire, albedo, and LAI were characterized by their arithmetic mean and standard deviation. Afterward, we calculated the Pearson correlation coefficient to estimate the relationships between albedo and response variables (i.e., LAI, precipitation, and the number of fire events, and burn severity) in each study region. Prior to the test, we made sure that the data follow a normal distribution by visually checking their Q-Q (quantile-quantile) plots (Ghasemi and Zahediasl, 2012). We tested the significance of correlation at the level of 99% ($\alpha = 0.01$) and reported their p -values. In addition, we spatially and temporally aggregated time series of LAI, albedo to monthly averages and the number of fire events to monthly sums for each study region before computation of the correlation test. Precipitation data was already in monthly resolution and was not aggregated. We also estimated the linear relationship between burn severity (dNBR) and albedo using Pearson correlation test. However, when analyzing the correlation between albedo and dNBR, we aggregated both albedo and dNBR for a period of three months (see Section 2.3.2). We calculated the correlation by extracting the mean albedo values in the three-month summer season after the fire event (from the same year as the fire event) in each pixel. The records with missing values were removed before conducting the statistical test. For temporal analyses of each study site, we estimated the correlation between albedo and LAI with the same approach that we used for each study region.

2.4.1. Breaks for additive seasonal and trend method

We calculated the date of the largest breakpoint happening in the time series of MODIS albedo from 2000 to 2016 separately for each of the four study sites. In the context of our study, a breakpoint is

defined as the largest significant change in the time series of albedo values and should be, in theory, linked to an identifiable environmental disturbance.

First, we decomposed the albedo time series into the trend and seasonal components (Verbesselt and Hyndman, 2010). The breakpoints were calculated to estimate the largest trend changes through time using the “breaks for additive seasonal and trend” (BFAST) method (Verbesselt and Hyndman, 2010). This method iteratively fits a piecewise linear trend and a seasonal model to the time series data (from time points 1 to n) using:

$$Y_t = T_t + S_t + e_t \quad t = 1, \dots, n \tag{5}$$

where Y_t is the observed data at time point t , T_t is the trend component, S_t is the seasonal component, and e_t is the remainder component (Verbesselt and Hyndman, 2010). It is assumed that T_t is a piecewise linear function with $m + 1$ segments. Each segment has a specific slope and intercept. Thus, there are m breakpoints $\tau_1^*, \dots, \tau_m^*$, such that:

$$\tau_{i-1}^* < t < \tau_i^* \tag{6}$$

where $i = 1, \dots, m$.

In this study, we used breakpoints of a trend at $\tau_1^*, \dots, \tau_m^*$ that can be estimated using the residuals-based moving sum test, and are assessed by minimizing a Bayesian information criterion (BIC) from the seasonally adjusted data $Y_t - \hat{S}_t$, where \hat{S}_t is first found by the STL method (Cleveland et al., 1990). Seasonal and Trend decomposition using LOESS (STL) is a filtering procedure for decomposing a seasonal time series into trend, seasonal, and residual components using a sequence of applications of the loess smoother.

The trend between breakpoints is given as:

$$\hat{T}_t = \hat{\alpha}_i + \hat{\beta}_j t \tag{7}$$

\hat{T}_t , $\hat{\alpha}_i$ and $\hat{\beta}_j$ are estimated using robust regression based on M-estimations (Verbesselt and Hyndman, 2010).

In our analysis, the number of breakpoints per time series was restricted to one, which was the largest significant breakpoint. After finding the breakpoint in the time series, we estimated the mean of albedo and LAI values 365 days before and 365 days after a breakpoint occurred.

3. Results

In this section, we first report analyses at the regional scale to get an overview of long-term climate change in the Middle East from 1950 to 2016. Then, we explore the spatio-temporal dynamics of albedo, LAI and disturbances (the number of fire events, burn severity and precipitation) in the Zagros Mountains. Later on, we focus on changes in albedo and LAI under influence of disturbances at the four study sites, located in different parts of the Zagros area.

3.1. Long-term changes in climate in the Middle East and Zagros area

At the regional level, the severe long-term drought was due to a precipitation shortage (up to 43 mm in mean monthly precipitation from 1950 to 2016) especially in Iran, Turkey and Iraq, where the Zagros forests spread (Fig. 2B). The precipitation anomaly co-occurred with a temperature anomaly (up to 4 °C increase in the monthly mean), potential evapotranspiration anomaly (up to 45 mm increase in the monthly mean) and highly frequent fire events (up to 17 events in one pixel from 2000 to 2016) in the Middle East (Fig. 2A, D). A visual comparison of the spatial distribution of the changes in the climate variables (Fig. 2) shows that the magnitude of change considerably varies along latitudes. The southern Zagros area showed large changes in climate variables, which were connected to the frequent occurrences of the fire events

during years 2000–2016 (Fig. 2D). Therefore, the results showed a precipitation shortage along with temperature, evapotranspiration and fire increases from 1950 to 2016 in the Middle East.

Next, we took a closer look at the time series of climate variables from 1950 to 2016 in our four study sites (Fig. 3). For the study period of 1950–2016, the mean values of temperature in Marivan and Ilam were 8 °C and 12 °C, respectively, while these values in Ize and Dashte baram were 19 °C and 21 °C. Similarly, the mean values of monthly precipitation in Marivan and Ilam were 76 mm and 37 mm, respectively, while these values in Ize and Dashte baram were 34 mm and 20 mm, respectively. Thus, the sites in southern Zagros (Dashte baram and Ize) were relatively warmer and drier than sites in the northern Zagros (Ilam and Marivan). In addition, the effects of ENSO were clear in the temporal dynamics of the climate variables in the study sites (Fig. 3); the changes in the occurrence of ENSO around 2007–2008 resulted in a historical record of the highest temperature in all study sites, and the precipitation anomaly during 1950–2016 (Fig. 3).

3.2. Spatio-temporal changes of albedo, LAI, and disturbances in the entire Zagros area

To get an overview of changes in albedo and LAI of Zagros area, we analyzed concurrent changes in MODIS albedo and LAI spatially throughout the Zagros forests (Fig. 4). The results showed that the

magnitude of change, obtained from the comparison of years between 2000 and 2002 with years 2014 to 2016 in both LAI and albedo had a gradient from east to west in the Zagros area. In general, the magnitude of change in albedo increased and that of LAI decreased towards the east (Fig. 4A, B).

On average, LAI values in the northern Zagros were slightly ($0.12 \text{ m}^2 \text{ m}^{-2}$) higher than in the southern Zagros (Fig. 5). This indicates that the northern Zagros was slightly greener than the southern Zagros. Albedo values, on the other hand, differed only marginally (0.002 units). Notably, the northern and the southern Zagros experienced their lowest LAI starting around 2007, when ENSO happened (Fig. 5). In addition, when comparing the relationship between the albedo and LAI in the northern and the southern Zagros using a correlation test, the results showed a strong inverse relationship between albedo and LAI. Lower LAI values resulted in higher albedo values (Table 2).

To link albedo dynamics with the number of fire events, burn severity and drought, we quantified the time series of mean monthly precipitation and total number of fire events per month from 2000 to 2016 in the northern and southern Zagros. In general, precipitation rate on average was the same in the northern and southern Zagros. However, the total number of fire events per month in the northern Zagros was slightly higher than in the southern Zagros from 2000 to 2016 (Table 3). Oppositely, the mean severity of fires in the southern Zagros was higher than in the northern Zagros. In both regions, the mean

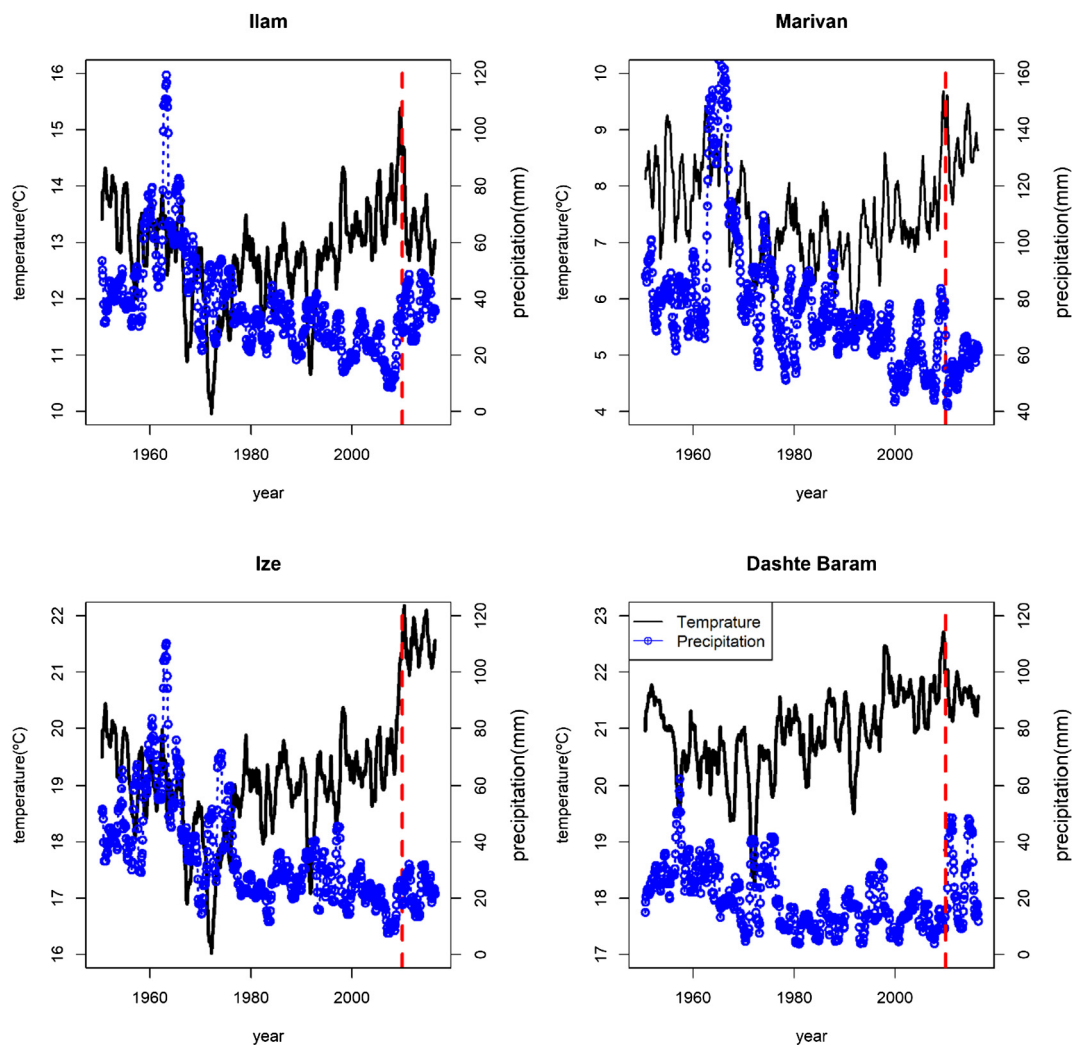


Fig. 3. Smoothed time-series of monthly temperature (°C) and precipitation (mm) in the four forest sites based on climate data since 1950 obtained from the FetchClimate website. Dashed blue lines with circles represent precipitation, and continuous black lines represent temperature. The red dashed line indicates the average time of the maximum-recorded temperature in all the study sites (i.e., August 2008). (For interpretation of the references to colour in this figure legend, the reader is referred to the web version of this article.)

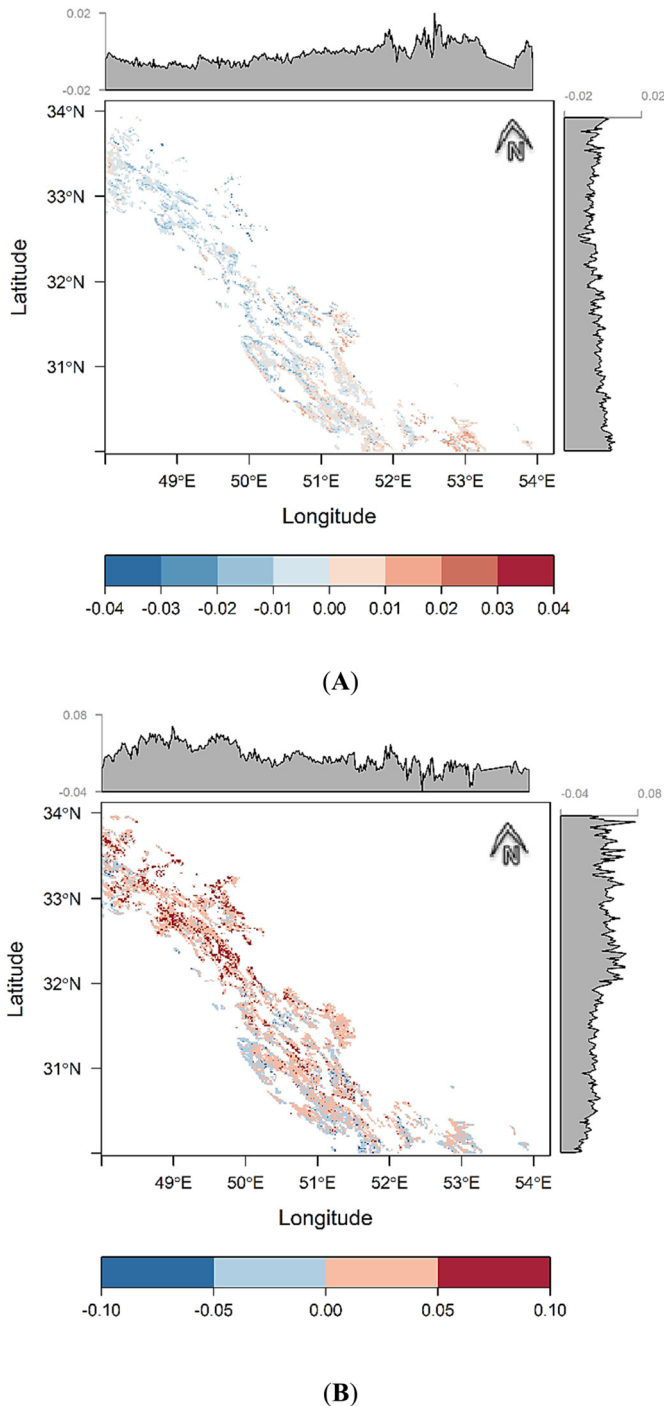


Fig. 4. A. Spatial distribution of the magnitude of change in albedo between the periods 2000 to 2002 and 2014 to 2016 in the Zagros sparse forests. B. Spatial distribution of the magnitude of change in LAI between the periods 2000 to 2002 and 2014 to 2016; the gray shades surrounding the figures represent the mean magnitude of change (A, B).

burn severity was moderate. The results of comparing the link between the albedo and the number of fire events in both areas using correlation test indicated a relatively strong inverse relationship. Nevertheless, the links between mean monthly precipitation and albedo, and between the burn severity and albedo (Appendix: Fig. A4) were fairly weak between 2000 and 2016 (Table 3). In addition, we estimated the correlation coefficient between the number of fire events and precipitation from 2000 to 2016. This may suggest that whether there is any interaction between these variables in explaining the albedo. The results showed a relatively weak but significant correlation (with a correlation coefficient of 0.31)

in the northern Zagros, and a non-significant correlation in the southern Zagros (with a correlation coefficient of -0.13).

3.3. Temporal changes in albedo and LAI in the four study sites

3.3.1. Estimation of albedo and LAI trends

According to the data on the quality of the MODIS albedo in the southern sites (i.e., Dashte baram, Ize), snow-covered pixels were rarely a problem (Appendix: Fig. A2, A3) whereas in the northern sites (i.e., Ilam, Marivan) snow covers were present every winter for a short period. In general, the percentage of high-quality retrievals of the remotely sensed albedo in all the sites was high (Appendix: Figs. A2, A3, Table 1). The percentage of the high-quality data in Ize and Dashte baram (the southern Zagros) was higher than in Marivan and Ilam (northern Zagros).

Overall, the time series of LAI values in the study sites represented clear fluctuations but with relatively low values (<0.65), which is common for woodlands, savannas and sparse forests ecosystems. Therefore, the changes in LAI that we examined were very small (Fig. 6).

The mean albedo values in the study sites ranged from 0.16 to 0.20 (Table 4). All the study sites showed a decrease in LAI in 2007, following the severest drought event (Fig. 3). Since 2000, LAI of all the study sites (except Dashte baram) slightly increased and albedo decreased. The correlations between LAI and albedo were relatively low in all four study sites ($|r| \leq 0.53$) (Table 4).

3.3.2. Breakpoints in albedo time series and changes in tree cover

We identified the most significant breakpoint of changes in the albedo time series using the BFAST method. Dashte baram and Marivan had their largest significant breakpoints in the albedo time series in 2007 and 2008, respectively. Ilam and Ize on the other hand, showed their largest breakpoints in 2013 and 2014, respectively, when a set of severe fires occurred in the study sites (Fig. 7).

Exploring the dynamics of albedo close to the breakpoint demonstrated that when the fire events were the main disturbance in Ilam and Ize, a slight decrease in mean albedo happened. However, when the drought was the main disturbance in Marivan and Dashte baram, a slight increase in mean albedo occurred (Table 5, Fig. 7). In addition, disturbances resulted in an LAI decrease in all study sites, except Dashte baram.

Finally, we analyzed the changes in tree cover close to the breakpoints (Table 6). Before the breakpoints, the tree cover in all study sites ranged from 46% to 50% (Table 6). After the breakpoints, the sites in the southern Zagros (Ize and Dashtebaram) experienced substantially larger tree cover losses compared to the northern Zagros.

4. Discussion

In this paper, we investigated the link between albedo dynamics and disturbance types in the Zagros area as well as in four study sites within the area. To link albedo with drought conditions in a forest ecosystem, we hypothesized that drought conditions will significantly increase the albedo. Our large-scale analyses showed that, indeed, there is a relatively weak, but significant correlation between albedo and precipitation (correlation coefficient -0.27 and -0.25 in the northern and southern Zagros respectively; Table 3). Furthermore, we investigated the link between drought and the largest significant albedo changes in our finer-scale analyses. The results demonstrated that the largest albedo change in Marivan and Dashte baram occurred around 2007–2008 (Fig. 7 and Table 5). The reason behind this phenomenon was most likely the occurrence of ENSO in the Middle East that caused a severe drought in Iran between 2007 and 2008, which abruptly affected the ecosystems in the region (Barlow et al., 2016; Hosseinzadeh Talaei et al., 2014; Trigo et al., 2010; Voss et al., 2013). Such increases in albedo have also been reported previously in Sahara (-0.06 increase in albedo) under the influence of drought conditions (Govaerts and

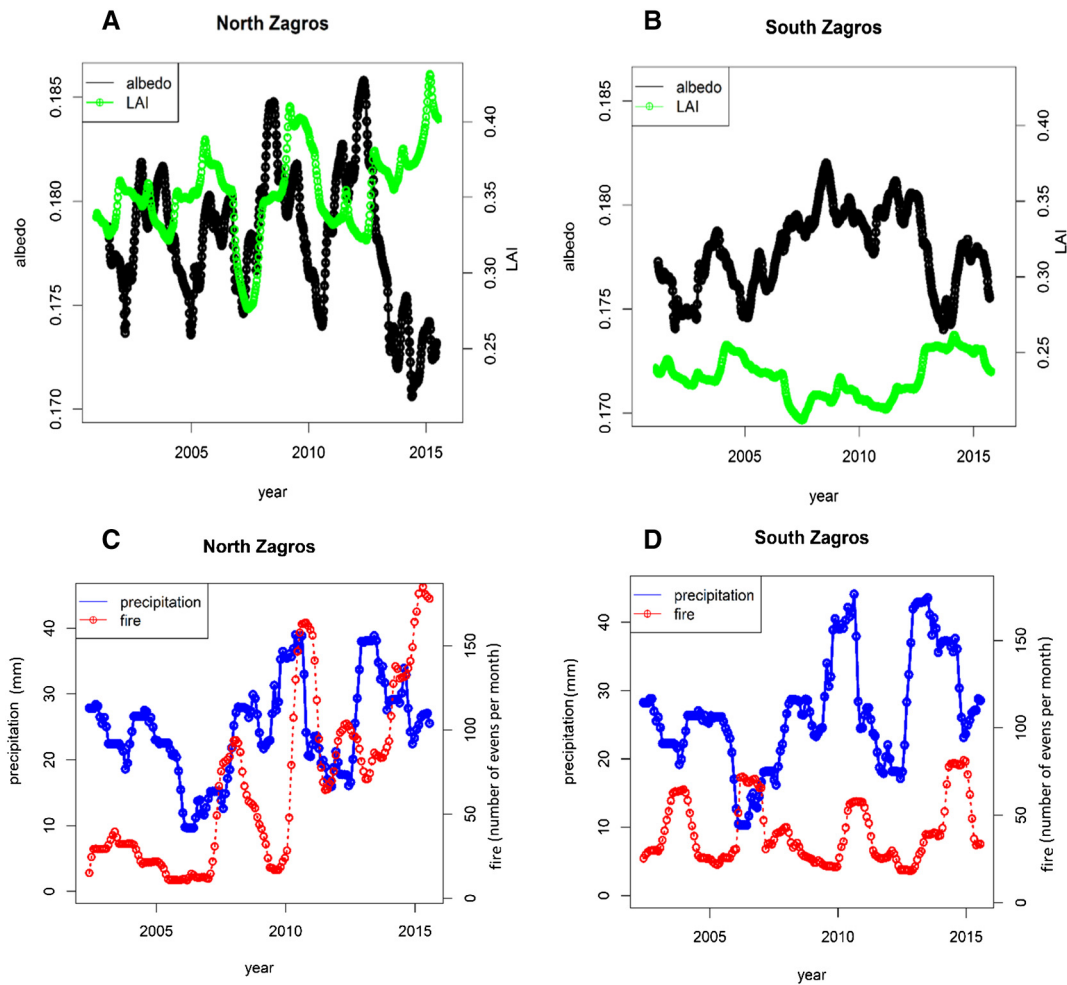


Fig. 5. A–B: Time series of albedo (black) and LAI (green) in northern and southern Zagros from 2000 to 2016; C–D: Time series of mean monthly precipitation (blue) and the number of fire events per month (red) in northern and southern Zagros from 2000 to 2016. (For interpretation of the references to colour in this figure legend, the reader is referred to the web version of this article.)

Table 2
Summary of albedo and LAI in the northern and the southern Zagros from 2000 to 2016.

Study regions	Number of pixels	Arithmetic mean in 2000–2016		Standard deviation in 2000–2016		Correlation coefficient
		Albedo	LAI	Albedo	LAI	Albedo & LAI
Northern Zagros	62,980	0.178	0.35	0.003	0.029	−0.74*
Southern Zagros	41,117	0.177	0.23	0.001	0.013	−0.69*

* The significance threshold was set at 0.01 using p-value; the star sign (*) refers to significant correlation test.

Lattanzio, 2008). The physical explanation is that drought can result in defoliation and canopy cover losses which, in turn, lead to changes in the visibility, spectral signature, and brightness of soils. Bare soils tend to be brighter than vegetation, and therefore, a decrease in vegetation

can translate into an increase in surface albedo (Govaerts and Lattanzio, 2007).

To link the number of fire events and albedo, we hypothesized that fire events will significantly reduce the albedo. Our large-scale analysis

Table 3
Summary of albedo versus the number of fire events per month, burn severity and mean monthly precipitation, aggregated (using the mean function) in the northern and the southern Zagros from 2000 to 2016.

Study region	Arithmetic mean Standard deviation in 2000–2016			Correlation coefficient	Correlation coefficient	Correlation coefficient
	Precipitation [mm per month]	Fire [Fire events per month] ^a	Burn severity (dNBR)	Precipitation & albedo	The number of fire events & albedo	Burn severity & albedo
Northern Zagros	24 7	64 51	0.31 0.20	−0.27*	−0.40*	0.18*
Southern Zagros	27 8	40 18	0.40 0.24	−0.25*	−0.59*	0.17

* The significance threshold was set at 0.01 using p-value; the star sign (*) refers to significant correlation test. The levels of burn severity are classified as low severity if it ranges between +0.1 to +0.27, moderate severity between +0.27 to +0.66, and high severity greater than +0.66.

^a Values from Fig. 5.

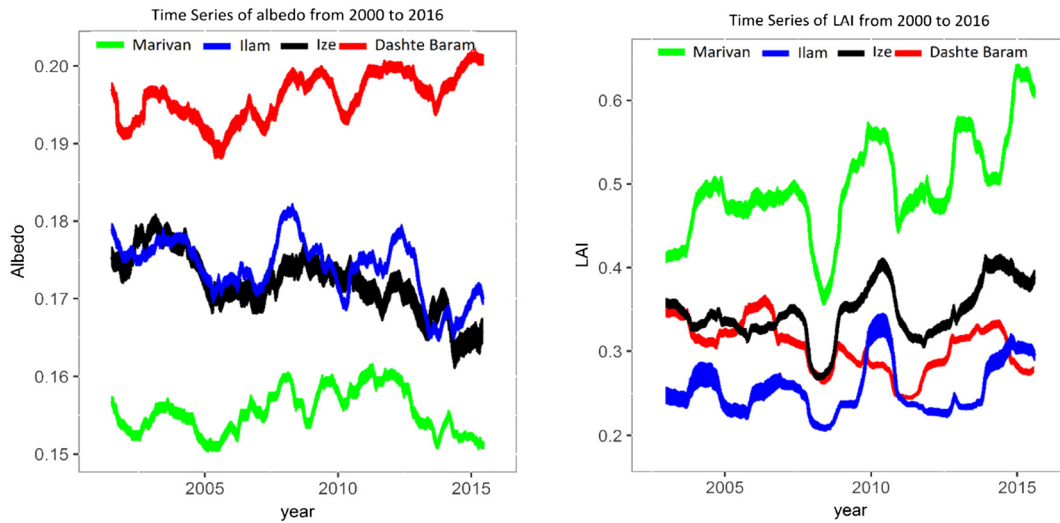


Fig. 6. Dynamics of albedo and LAI in the four study sites from 2000 to 2016 based on MODIS data. The line thickness represents the range of values over the pixels.

indicated a relatively strong inverse relationship, with a significant correlation of -0.40 , and -0.59 in the northern and southern Zagros, respectively (Table 3). In addition, the analyses in the study sites demonstrated that Ilam and Ize sites had the largest albedo change after a fire event in 2013–2014 (Fig. 7 and Table 5). A previous study reported a similar decrease in albedo (by 0.02) after a wildfire in a savanna type forest in northern Australia (Jin and Roy, 2005). This is probably because the black carbon that remains from a fire event stays on the ground, thus absorbing more incoming radiation. Noteworthy, we speculate that in the Zagros area, the remaining charcoals on the ground are not long-lasting, since the albedo is linked to the number of fire events with a relatively strong correlation coefficient, while its correlation with burn severity is relatively weak (Table 3). In boreal forests, charcoals can vanish due to snow or instantaneous early succession vegetation replacement (Amiro et al., 2006; Lyons et al., 2008). In the Zagros area, low rates of annual precipitation after the fires (breakpoints) in Ilam and Ize have been observed (Fig. 3). On the other hand, the average burn severity is only moderate in the Zagros area (Table 3), and therefore, the fire events could have helped plant growth by increasing soil fertility (Fattahi and Ildoromi, 2011; Heydari et al., 2017). Hence, vanishing of coals in the Zagros area can be due to fast vegetation regrowth. The effects of black carbon on albedo or low post-fire albedo have been reported previously in e.g. Greece (Veraverbeke et al., 2010a) and Africa (Dintwe et al., 2017). Opposite to semiarid sparse forests, albedo tends to increase after fire events in the boreal region (O'Halloran et al., 2012). The increases in albedo after a fire event in the boreal zone has often been explained by snowfall (Liu et al., 2005; Lyons et al., 2008).

Although many studies have been dedicated to characterizing the links between fire events and surface albedo, the effects of burn severity

on the changes of surface albedo are less known (Jin et al., 2012). In this study, we showed that the burn severity weakly (but significantly) explained the albedo with a correlation of 0.18 in the northern Zagros, and 0.17 in the southern Zagros (Table 3). The reason behind this weak relationship is probably related to the complex mechanism of vegetation dynamics in the Zagros area (see the following paragraphs for more details). Using field plots in the Zagros area, a study showed that the different degrees of burn severity caused differing vegetation responses, thus making the prediction of fire influences on vegetation complicated and impossible to extrapolate from one ecosystem to another (Pourreza et al., 2014). In this study, we hypothesized that the dynamics of albedo is affected by major vegetation changes. Our large-scale analyses represented a strong inverse relationship between albedo and LAI with correlation -0.74 and -0.69 in the northern and southern Zagros, respectively (Fig. 5 Table 2). The analyses of the study sites showed again an inverse relationship, but with weaker correlations compared to the large-scale results (Fig. 6, Table 4). Previous studies have also shown that such an inverse relationship between LAI and albedo in the boreal zone (Lukeš et al., 2013). A number of physical mechanisms can explain the link between vegetation and albedo. First, vegetation can determine a surface roughness, and a decrease in roughness, associated with drought, can result in an albedo change. On the other hand, active vegetation cover by absorbing photosynthetically active wavelengths (400–700 nm) has a dual role in albedo; the higher the tree cover, the lower the albedo. Such processes are assumed as important mechanisms in semiarid regions (Charney, 1975). Another mechanism is related to the dynamics of ecosystems: ENSO led to a decrease in LAI in the Zagros forests in 2007 that was recovered in a year in the northern Zagros while it took approximately 6 years to recover in the southern part (Fig. 6).

Such difference in vegetation dynamics in the northern and southern Zagros areas is most likely due to two reasons. Firstly, studies showed relationships between the level of water stress in a forest ecosystem and the severity of the fungi and beetle attacks effects on oak forests (Capretti and Battisti, 2007; Linaldeddu et al., 2011; Vannini et al., 2009). Therefore, the effects from beetle and fungal attacks in areas with higher precipitation (e.g. in Ilam and Marivan) may be smaller than in areas with lower mean precipitation (e.g. in Dashte baram and Ize) (Fig. 3). Secondly, based on the albedo, LAI and dNBR changes observed in this study, we can assume that the wildfires in Marivan were moderate. Moderate fire events can result in a higher availability of phosphorus, nitrate nitrogen, potassium, and acidity (Fattahi and Ildoromi, 2011; Heydari et al., 2017). As soil fertility is often a problem for plant growth in the northern Zagros area, the fire

Table 4
Albedo and LAI in the study sites for the time of period 2000–2016.

Study site	Arithmetic mean in 2000–2016		Standard deviation in 2000–2016		Correlation coefficient
	Albedo	LAI	Albedo	LAI	
Marivan	0.157	0.528	0.002	0.058	+0.27*
Ilam	0.179	0.255	0.003	0.029	-0.51*
Ize	0.173	0.345	0.003	0.032	-0.20*
Dashte baram	0.199	0.304	0.004	0.029	-0.53*

* The significance threshold was set at 0.01 using p -value; the star sign (*) refers to significant correlation test.

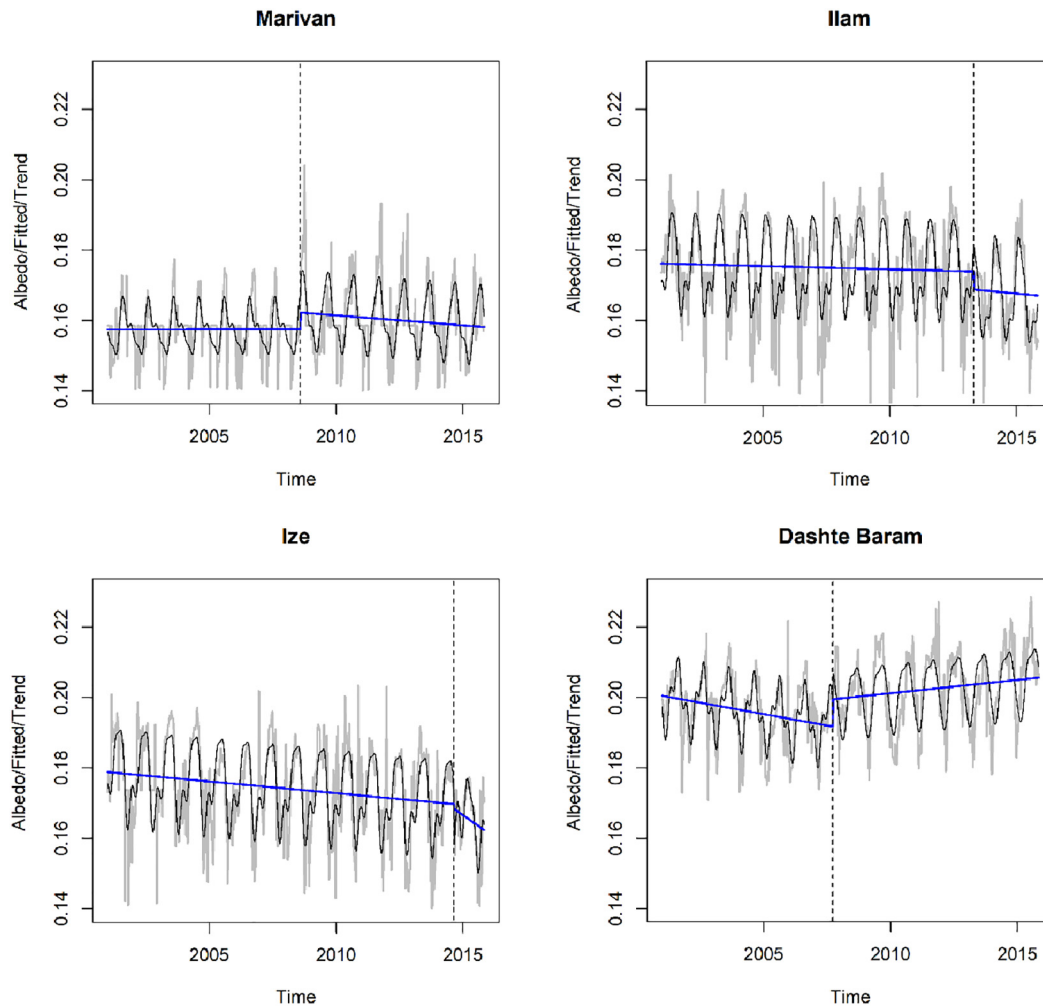


Fig. 7. Breakpoints in MODIS albedo time series in the four study sites based on the BFAST method. The black line is the fitted model, the blue line is the trend, and gray lines are the actual data. The dashed vertical line indicates the date of the breakpoint. (For interpretation of the references to colour in this figure legend, the reader is referred to the web version of this article.)

events could have helped plant growth by increasing soil fertility (Fattahi and Ildoromi, 2011; Heydari et al., 2017). This phenomenon can also explain the positive correlation between albedo and LAI in Marivan (Table 4). When tree cover has been reduced by disturbances (Table 6), the LAI has increased in Marivan (Table 5), that could be related to the understory. Furthermore, our results revealed that vegetation in the Dashte baram has become greener in 2007 (Table 5), even though the tree cover decreased. We should, however, note that first, the magnitude of change in LAI is still very small; and second, the increase in LAI is most likely due to an increase of the vegetation in the herb and grass layers, not an increase in the tree cover. This is supported by our analysis of tree cover changes using high spatial resolution satellite data: tree cover loss due to the disturbances varied, from +2 to −17% (Table 6). Previously, tree cover losses in the Zagros area have been reported also by (Henareh Khalyani and Mayer, 2013; Sadeghi

et al., 2017). Analyzing the link between satellite-based albedo and LAI in sparse forest (or woodland) ecosystems is not trivial: the total LAI may increase even though the area is going through major losses in the tree cover, which in turn changes the microclimate of the forest areas.

Due to the current political situation, accessing field data from the Middle East is difficult, and thus the common understanding of climate change in the region is strongly based on satellite data. Continuous field measurements on forest structure and detailed information on the magnitude of forest disturbances would, nevertheless, help to determine the climate impacts of various ecosystem disturbance more accurately. For example in Iran, there has been no update on changes in forests (even at a coarse spatial resolution) since 2011 (Abbaspour et al., 2009). Using coarse resolution satellite products (such as the MODIS albedo and LAI products) to look at changes in forests also introduces

Table 5

The timing of breakpoints in albedo time series in the four study sites, and the change in albedo after breakpoint i.e., the mean difference in albedo and LAI between periods of 365 days before and after a breakpoint occurred.

Study site	Breakpoint [t]	Albedo change	LAI change
Marivan	July 2008	+0.002	−0.010
Ilam	October 2013	−0.013	−0.020
Ize	August 2014	−0.028	−0.028
Dashte baram	September 2007	+0.004	+0.017

Table 6

Tree cover values in study sites before and after the albedo breakpoint.

Study site	Tree cover (before)	Tree cover (after)	Gain/loss in tree cover	Standard error
Marivan	0.50	0.48	−0.02	0.024
Ilam	0.46	0.47	+0.02	0.023
Ize	0.48	0.31	−0.17	0.021
Dashte baram	0.46	0.30	−0.16	0.024

uncertainties related to forest heterogeneity: a large pixel may include several types (or densities) of forests. In this study, we assumed that the vegetation structure was relatively homogeneous within each MODIS pixel. This was supported also by the data: all pixels in each site showed relatively similar changes throughout the study period from 2000 to 2016 (as indicated by the line thickness in Fig. 6). In addition, it is worth to mention that in this study, by comparing the data from fire stations and local reports with the fire events obtained from the satellite products (results not shown), we noticed that some of the fires were not detected by the satellite product (i.e., FIRMS) in the study sites. According to the local fire station data (Allahdeh et al., 2014), only 30% of the fires have been detected by the MODIS products in the Zagros area. This might be because of the short time period of some fires, i.e., they may have started and ended between satellite overpasses, or were obscured due to cloud cover, heavy smoke, or dense tree canopy. In addition, specifically in the Zagros area, this might also be related to the coarse spatial resolution (1-km) of the FIRMS product, and the algorithm that captures only large fires. Another reason could be related to the low fire temperature in these areas (Allahdeh et al., 2014). Some studies identified phenology as a confounding factor for mapping the burn severity using dNBR (Verbyla et al., 2008), and that can also be considered as a source of uncertainty. The dNBR values are strongly correlated with pre-fire green biomass because areas with the greatest absolute difference between pre- and post-fire vegetation covers can achieve the highest dNBR values (Miller and Thode, 2007). Accordingly, if two areas with different pre-fire vegetation covers experience a stand-replacing fire, each could be assigned to a different burn severity class. Finally, it should be noted that for ecosystems with very low LAI values, as in our study, interpretation of marginal changes in the time series could be challenging due to uncertainties in the original satellite product.

In general, previous studies have shown the significant drought condition starting from 1960 in the Middle East: temperatures have increased by 3.5 °C to 7 °C, and there has been a 10% higher variability in natural precipitation (Kaniewski et al., 2012; Lelieveld et al., 2012). Simultaneously, wide mortality of oak trees has been reported from 1980 onwards in the Mediterranean basin (da Clara, 2013) and oak forests in Iran, Turkey, and Iraq (Henareh Khalyani and Mayer, 2013; Sadeghi et al., 2017). In this study, our results confirmed that the Middle East is still facing a precipitation shortage and ever-higher temperatures, especially in northern Turkey and the Zagros area (Fig. 2).

5. Conclusions

From the perspective of linking albedo changes to natural forest disturbances, we illustrated that the changes in vegetation, precipitation, the number of fire events, and burn severity can explain albedo dynamics through expectedly an inverse relationship. In addition, the number of fire events is strongly linked to the albedo in Zagros. Furthermore, we showed that LAI slightly increased since 2000 in some areas in the Zagros forests, which is most likely due to an increase of the vegetation in the herb- and grass-layers, not an increase in tree covers. In addition, our analysis showed that the Middle East is still facing a continuous drought condition.

Acknowledgments

This work was partly supported by Academy of Finland [grant 13286390]. We acknowledge Dr. Terhikki Manninen (Finnish Meteorological Institute, Helsinki, Finland) for her comments on the manuscript at its different phases. In addition, we thank our colleagues Dr. Hadi [Aalto University, Geoinformatics group, Finland] who provided insight that greatly assisted the research. Dr. Bakhtiar Fattahi (Assistant Professor, Faculty of Natural Resources and Environment, Malayer University, Iran) for forest fire reports, and Dr. Shahram Ahmadi (Senior expert at Department of natural resources in Fars, Iran), Ahmad Hossein Zade

(MSc, Faculty of Forestry, Gheir Entefai University, Ilam, Iran) and Mohammad Jabari (MSc, Faculty of Environmental Science, Daneshgah Azade Eslami, Tehran, Iran) for background information on study sites in Zagros area. We acknowledge the use of data and imagery from LANCE FIRMS operated by the NASA/GSFC/Earth Science Data and Information System (ESDIS) with funding provided by NASA/HQ (<https://Earthdata.nasa.gov/Earth-observation-data/near-real-time/citation#ed-lance-disclaimer>). In addition, we acknowledge NCEP Reanalysis data provided by the NOAA/OAR/ESRL PSD, Boulder, Colorado, USA, from their Web site at <http://www.esrl.noaa.gov/psd/> and CESM1-BGC model output prepared for CMIP5 rcp85.

Appendix A. Supplementary data

Supplementary data to this article can be found online at <https://doi.org/10.1016/j.scitotenv.2019.01.253>.

References

- Abbaspour, K.C., Faramarzi, M., Ghasemi, S.S., Yang, H., 2009. Assessing the impact of climate change on water resources in Iran. *Water Resour. Res.* 45.
- Abera, T.A., Heiskanen, J., Pellikka, P., Rautiainen, M., Maeda, E.E., 2019. Clarifying the role of radiative mechanisms in the spatio-temporal changes of land surface temperature across the Horn of Africa. *Remote Sens. Environ.* 221, 210–224.
- Alkama, R., Cescatti, A., 2016. Biophysical climate impacts of recent changes in global forest cover. *Science* 351, 600–604. <https://doi.org/10.1126/science.aac8083> (80-).
- Allahdeh, P., Darvishsfat, Zadeegan, S., Pedram, A., 2014. Application of MODIS algorithm to detect Zagros forest fire. *For. Wood J.* 67, 201–213 URL https://jfwup.ut.ac.ir/article_51541.html (Persian Language).
- Amiro, B.D., Orchansky, A.L., Barr, A.G., Black, T.A., Chambers, S.D., Chapin Iii, F.S., Goulden, M.L., Litvak, M., Liu, H.P., McCaughey, J.H., 2006. The effect of post-fire stand age on the boreal forest energy balance. *Agric. For. Meteorol.* 140, 41–50.
- Arekhi, Saleh, 2011. Modeling spatial pattern of deforestation using GIS and logistic regression: a case study of northern Ilam forests, Ilam province, Iran. *African J. Biotechnol.* 10, 16236–16249. <https://doi.org/10.5897/AJB11.1122>.
- Arsalani, A., Azizi, G., Bräuning, A., 2015. Dendroclimatic reconstruction of May–June maximum temperatures in the central Zagros Mountains, western Iran. *Int. J. Climatol.* 35, 408–416. <https://doi.org/10.1002/joc.3988>.
- Azizi, G., Arsalani, M., Bräuning, A., Moghimi, E., 2013. Precipitation variations in the central Zagros Mountains (Iran) since A.D. 1840 based on oak tree rings. *Palaeogeogr. Palaeoclimatol. Palaeoecol.* 386, 96–103. <https://doi.org/10.1016/j.palaeo.2013.05.009>.
- Barlow, M., Zaitchik, B., Paz, S., Black, E., Evans, J., Hoell, A., 2016. A review of drought in the Middle East and southwest Asia. *J. Clim.* 29, 8547–8574. <https://doi.org/10.1175/JCLI-D-13-00692.1>.
- Bazyar, M., Haidari, M., Shabanian, N., Haidari, R.H., 2013. Impact of physiographical factors on the plant species diversity in the Northern Zagros Forest (Case study, Kurdistan Province, Marivan region). *Ann. Biol. Res.* 4, 317–324.
- Bonan, G.B., 2008. Forests and climate change: forcings, feedbacks, and the climate benefits of forests. *Science* 320, 1444–1449. <https://doi.org/10.1126/science.1155121> (80-).
- Bright, R.M., Davin, E., O'Halloran, T., Pongratz, J., Zhao, K., Cescatti, A., 2017. Local temperature response to land cover and management change driven by non-radiative processes. *Nat. Clim. Chang.* 7, 296.
- Bright, R.M., Zhao, K., Jackson, R.B., Cherubini, F., 2015. Quantifying surface albedo and other direct biogeophysical climate forcing of forestry activities. *Glob. Chang. Biol.* 21, 3246–3266. <https://doi.org/10.1111/gcb.12951>.
- Capretti, P., Battisti, A., 2007. Water stress and insect defoliation promote the colonization of *Quercus cerris* by the fungus *Biscogniauxia mediterranea*. *For. Pathol.* 37, 129–135.
- Chambers, S.D., Chapin, F.S., 2002. Fire effects on surface-atmosphere energy exchange in Alaskan black spruce ecosystems: implications for feedbacks to regional climate. *J. Geophys. Res.* 108, 8145. <https://doi.org/10.1029/2001JD000530>.
- Charney, J.G., 1975. Dynamics of deserts and drought in the Sahel. *Q. J. R. Meteorol. Soc.* 101, 193–202. <https://doi.org/10.1002/qj.49710142802>.
- Cleveland, R.B., Cleveland, W.S., McRae, J.E., Terpenning, I., 1990. STL: a seasonal-trend decomposition procedure based on loess. *J. Off. Stat.* 6, 3–73. <https://doi.org/citeulike-article-id:1435502>.
- da Clara, P.E., 2013. Decline of mediterranean oak trees and its association with *Phytophthora cinnamomi*: a review. *Eur. J. For. Res.* 132, 411–432.
- Dintwe, K., Okin, G.S., Xue, Y., 2017. Fire-induced albedo change and surface radiative forcing in sub-Saharan Africa savanna ecosystems: implications for the energy balance. *J. Geophys. Res. Atmos.* 122, 6186–6201. <https://doi.org/10.1002/2016JD026318>.
- Doubek, J., 2013. Zagros Folded Zone. URL https://en.wikipedia.org/wiki/Zagros_Mountains#/media/File:Zagros_Folded_Zone.jpg (Accessed: 17.12.2018).
- FAO, 2003. Organization, Food and Agriculture. URL <http://www.fao.org/english/news-room/news/2003/21962-en.html> (Accessed: 17.12.2018).
- Fathizadeh, O., Hosseini, S.M., Zimmermann, A., Keim, R.F., Darvishi Bolorani, A., 2017. Estimating linkages between forest structural variables and rainfall interception parameters in semi-arid deciduous oak forest stands. *Sci. Total Environ.* 601–602, 1824–1837. <https://doi.org/10.1016/j.scitotenv.2017.05.233>.
- Fattahi, B., Ildoromi, A.R., 2011. Effect of some environmental factors on plant species diversity in the mountainous grasslands (case study: Hamedan - Iran). *Int. J. Nat. Resour. Mar. Sci.* 1, 45–52.

- FIRMS, 2018. Fire Information for Resource Management System. URL: <https://doi.org/10.5067/FIRMS/MODIS/MCD14DLNRT.006> (Accessed: 17.12.2018).
- Fleming, M.D., Hoffer, R.M., 1979. Machine Processing of Landsat MSS data and DMA Topographic Data for Forest Cover Type Mapping. LARS Technical Reports 062879, p. 80.
- Gatebe, C.K., Ichoku, C.M., Poudyal, R., Román, M.O., Wilcox, E., 2014. Surface albedo darkening from wildfires in northern sub-Saharan Africa. *Environ. Res. Lett.* 9, 65003.
- GCOS, 2006. Systematic Observation Requirements for Satellite-based Products for Climate-Supplemental Details to the Satellite-based Component of the "Implementation Plan for the Global Observing System for Climate in Support of the UNFCCC". Technical Report GCOS-107, WMO/TD No 1338.
- GFW, 2014. Watch. Glob. For.. URL: <http://www.globalforestwatch.org/> (Accessed: 01.01.2017).
- Ghasemi, A., Zahedi, S., 2012. Normality tests for statistical analysis: a guide for non-statisticians. *Int. J. Endocrinol. Metab.* 10, 486. <https://doi.org/10.5812/ijem.3505>.
- Giglio, L., Desloires, J., Justice, C.O., Kaufman, Y.J., 2003. An enhanced contextual fire detection algorithm for MODIS. *Remote Sens. Environ.* 87, 273–282. [https://doi.org/10.1016/S0034-4257\(03\)00184-6](https://doi.org/10.1016/S0034-4257(03)00184-6).
- Giglio, L., Schroeder, W., Justice, C.O., 2016. The collection 6 MODIS active fire detection algorithm and fire products. *Remote Sens. Environ.* 178, 31–41. <https://doi.org/10.1016/j.rse.2016.02.054>.
- Giorgi, F., Lionello, P., 2008. Climate change projections for the Mediterranean region. *Glob. Planet. Chang.* 63, 90–104. <https://doi.org/10.1016/j.gloplacha.2007.09.005>.
- Citas, I., Mitri, G., Veraverbeke, S., Polychronaki, A., 2012. Advances in remote sensing of post-fire vegetation recovery monitoring—a review. *Remote Sensing of Biomass—Principles and Applications*, pp. 144–176. URL: <https://www.intechopen.com/download/pdf/33854> (Accessed 20.12.2018).
- Govaerts, Y., Lattanzio, A., 2008. Estimation of surface albedo increase during the eighties Sahel drought from Meteosat observations. *Glob. Planet. Chang.* 64, 139–145. <https://doi.org/10.1016/j.gloplacha.2008.04.004>.
- Govaerts, Y., Lattanzio, A., 2007. Surface albedo response to Sahel precipitation changes. *EOS (Washington, DC)* 88, 25–26. <https://doi.org/10.1029/2007EO030002>.
- Grechka, D.A., Berezin, S.B., Emmott, S., Lyutsarev, V., Smith, M.J., Purves, D.W., 2016. Universal, easy access to geotemporal information: FetchClimate. *Ecography (Cop.)* 39, 904–911. <https://doi.org/10.1111/ecog.02321>.
- Hansen, M.C., Potapov, P.V., Moore, R., Hancher, M., Turubanova, S.A., Tyukavina, A., Thau, D., Stehman, S.V., Goetz, S.J., Loveland, T.R., Kommareddy, A., Egorov, A., Chini, L., Justice, C.O., Townsend, J.R.G., 2013. High-resolution global maps of 21st-century forest cover change. *Science* 342, 850–853. <https://doi.org/10.1126/science.1244693> (80-).
- Henareh Khalyani, A., Mayer, A.L., 2013. Spatial and temporal deforestation dynamics of Zagros forests (Iran) from 1972 to 2009. *Landscape Urban Plan.* 117, 1–12. <https://doi.org/10.1016/j.landurbplan.2013.04.014>.
- Henareh Khalyani, A., Mayer, A.L., Falkowski, M.J., Muralidharan, D., 2013. Deforestation and landscape structure changes related to socioeconomic dynamics and climate change in Zagros forests. *J. Land Use Sci.* 8, 321–340. <https://doi.org/10.1080/1747423X.2012.667451>.
- Heshmati, G.A., 2007. Vegetation characteristics of four ecological zones of Iran. *Int. J. Plant Prod.* 1 (2), 215–224. <https://doi.org/10.22069/ijpp.2012.538>.
- Heydari, M., Faramarzi, M., Pothier, D., 2016. Post-fire recovery of herbaceous species composition and diversity, and soil quality indicators one year after wildfire in a semi-arid oak woodland. *Ecol. Eng.* 94, 688–697. <https://doi.org/10.1016/j.ecoleng.2016.05.032>.
- Heydari, M., Rostamy, A., Najafi, F., Dey, D.C., 2017. Effect of fire severity on physical and biochemical soil properties in Zagros oak (*Quercus brantii* Lindl.) forests in Iran. *J. For. Res.* 28, 95–104. <https://doi.org/10.1007/s11676-016-0299-x>.
- Hijmans, R.J., 2017. Raster: Geographic Data Analysis and Modeling. R Package Version. URL: <https://CRAN.R-project.org/package=raster> (Access: 20.12.2018).
- Hosseinzadeh Talaei, P., Tabari, H., Sobhan Ardakani, S., 2014. Hydrological drought in the west of Iran and possible association with large-scale atmospheric circulation patterns. *Hydrol. Process.* 28, 764–773. <https://doi.org/10.1002/hyp.9586>.
- Hurrell, J.W., Holland, M.M.M., Gent, P.R., Ghan, S., Kay, J.E., Kushner, P.J., Lamarque, J.-F.F., Large, W.G.G., Lawrence, D., Lindsay, K., Lipscomb, W.H., Long, M.C., Mahowald, N., Marsh, D.R., Neale, R.B., Rasch, P., Vavrus, S., Vertenstein, M., Bader, D., Collins, W.D.D., Hack, J.J.J., Kiehl, J., Marshall, S., 2013. The community earth system model: a framework for collaborative research. *Bull. Am. Meteorol. Soc.* 94. <https://doi.org/10.1175/BAMS-D-12-00121> 130204122247009.
- IPCC, 2018. Fifth Assessment Report of the Intergovernmental Panel on Climate Change. URL: https://www.ipcc.ch/site/assets/uploads/2018/02/WG1AR5_all_final.pdf (Accessed: 20.12.2018).
- IUCN, 2001. The 2000 IUCN Red List of Threatened Species. URL: <https://www.iucnredlist.org/search?query=zagros&searchtype=species> (Accessed: 20.12.2018).
- Jarvis, A., Reuter, H.I., Nelson, A., Guevara, E., 2008. Hole-filled SRTM for the Globe Version 4. Available from CGIAR-CSI SRTM 90m Database. URL: <http://srtm.csi.cgiar.org> (Accessed: 17.12.2018).
- Jin, Y., Randerson, J.T., Goetz, S.J., Beck, P.S.A., Loranty, M.M., Goulden, M.L., 2012. The influence of burn severity on postfire vegetation recovery and albedo change during early succession in north American boreal forests. *J. Geophys. Res. Biogeosci.* 117. <https://doi.org/10.1029/2011JG001886>.
- Jin, Y., Roy, D.P., 2005. Fire-induced albedo change and its radiative forcing at the surface in northern Australia. *Geophys. Res. Lett.* 32, 1–4. <https://doi.org/10.1029/2005GL022822>.
- Kalnay, E., Kanamitsu, M., Kistler, R., Collins, W., Deaven, D., Gandin, L., Iredell, M., Saha, S., White, G., Woollen, J., Zhu, Y., Chelliah, M., Ebisuzaki, W., Higgins, W., Janowiak, J., Mo, K.C., Ropelewski, C., Wang, J., Leetmaa, A., Reynolds, R., Jenne, R., Joseph, D., 1996. The NCEP/NCAR 40-year reanalysis project. *Bull. Am. Meteorol. Soc.* 77, 437–471. [https://doi.org/10.1175/1520-0477\(1996\)077<0437:TNYRP>2.0.CO;2](https://doi.org/10.1175/1520-0477(1996)077<0437:TNYRP>2.0.CO;2).
- Kaniewski, D., Van Campo, E., Weiss, H., 2012. Drought is a recurring challenge in the Middle East. *Proc. Natl. Acad. Sci.* 109, 3862–3867. <https://doi.org/10.1073/pnas.1116304109>.
- Keenan, R.J., Reams, G.A., Achard, F., de Freitas, J.V., Grainger, A., Lindquist, E., 2015. Dynamics of global forest area: results from the FAO global forest resources assessment 2015. *For. Ecol. Manag.* 352, 9–20. <https://doi.org/10.1016/j.foreco.2015.06.014>.
- Key, C.H., Benson, N.C., 2006. Landscape Assessment (LA). FIREMON: Fire Effects Monitoring and Inventory System. Gen. Tech. Rep. RMRS-GTR-164-CD. page A427. URL: https://www.fs.fed.us/rm/pubs/rmrs_gtr164.pdf (Accessed: 18.12.2018).
- Knyazikhin, Y., Martonchik, J.V., Myneni, R.B., Diner, D.J., Running, S.W., 1998. Synergistic algorithm for estimating vegetation canopy leaf area index and fraction of absorbed photosynthetically active radiation from MODIS and MISR data. *J. Geophys. Res. Atmos.* 103, 32257–32275. <https://doi.org/10.1029/98JD02462>.
- Kolahi-Azar, A.P., Golriz, S., 2018. Multifractal topography: a tool to measure tectonic complexity in the Zagros Mountain range. *Math. Geosci.* 50, 431–445. <https://doi.org/10.1007/s11004-017-9720-z>.
- Kurz, W.A., Stinson, G., Rampley, G.J., Dymond, C.C., Neilson, E.T., 2008. Risk of natural disturbances makes future contribution of Canada's forests to the global carbon cycle highly uncertain. *Proc. Natl. Acad. Sci.* 105, 1551–1555. <https://doi.org/10.1073/pnas.0708133105>.
- Lamigueiro, O.P., Hijmans, R., 2018. rasterVis. R Package Version 0.44. URL: <http://oscarperpinan.github.io/rastervis> (Access: 20.12.2018).
- Landuse Map, 2000. URL: http://girs.ir/j%D88%A87%D89%87-9_%D88%A87%D88%B81%D88%A88%D88%B81%D88%A87%D88%B81%D88%A87%D88%B86%D88%A87%D88%B81%D88%A87%D89%86/ (Accessed: 01.01.2017).
- Lanorte, A., Danese, M., Lasaponara, R., Murgante, B., 2013. Multiscale mapping of burn area and severity using multisensor satellite data and spatial autocorrelation analysis. *Int. J. Appl. Earth Obs. Geoinf.* 20, 42–51. <https://doi.org/10.1016/j.jag.2011.09.005>.
- Lelieveld, J., Hadjinicolaou, P., Kostopoulou, E., Chenoweth, J., El Maayar, M., Giannakopoulos, C., Hannides, C., Lange, M.A., Tanarhte, M., Tyrilis, E., Koplaki, E., 2012. Climate change and impacts in the Eastern Mediterranean and the Middle East. *Clim. Chang.* 114, 667–687. <https://doi.org/10.1007/s10584-012-0418-4>.
- Lelieveld, J., Proestus, Y., Hadjinicolaou, P., Tanarhte, M., Tyrilis, E., Zittis, G., 2016. Strongly increasing heat extremes in the Middle East and North Africa (MENA) in the 21st century. *Clim. Chang.* 137, 245–260. <https://doi.org/10.1007/s10584-016-1665-6>.
- Linaldeddu, B.T., Sirca, C., Spano, D., Franceschini, A., 2011. Variation of endophytic cork oak-associated fungal communities in relation to plant health and water stress. *For. Pathol.* 41, 193–201. <https://doi.org/10.1111/j.1439-0329.2010.00652.x>.
- Lindgren, B.W., 1966. *Introduction to Probability and Statistics*, by BW Lindgren, and GW McElrath.
- Liu, H., Randerson, J.T., Lindfors, J., Chapin, F.S., 2005. Changes in the surface energy budget after fire in boreal ecosystems of interior Alaska: an annual perspective. *J. Geophys. Res. Atmos.* 110. <https://doi.org/10.1029/2004JD005158>.
- Lukeš, P., Stenberg, P., Rautiainen, M., 2013. Relationship between forest density and albedo in the boreal zone. *Ecol. Model.* 261–262, 74–79. <https://doi.org/10.1016/j.ecolmodel.2013.04.009>.
- Lyons, E.A., Jin, Y.F., Randerson, J.T., 2008. Changes in surface albedo after fire in boreal forest ecosystems of interior Alaska assessed using MODIS satellite observations. *J. Geophys. Res.* 113. <https://doi.org/10.1029/2007JG000606>.
- Ma, Q., 2008. The Status and Trends of Forests and Forestry in West Asia. Subregional Report of the Forestry Outlook Study for West and Central Asia. Forestry Policy and Institutions Working Paper (FAO).
- Majasalmi, T., Rautiainen, M., Stenberg, P., Manninen, T., 2015. Validation of MODIS and GEOV1 fPAR products in a boreal forest site in Finland. *Remote Sens.* 7, 1359–1379. <https://doi.org/10.3390/rs70201359>.
- Miller, J.D., Thode, A.E., 2007. Quantifying burn severity in a heterogeneous landscape with a relative version of the delta Normalized Burn Ratio (dNBR). *Remote Sens. Environ.* 109, 66–80. <https://doi.org/10.1016/j.rse.2006.12.006>.
- Mirabolfothy, M., 2013. Outbreak of charcoal disease on quercus spp and zalkova carpinifolia trees in forests of zagros and alborz mountains in Iran. *Iranian J Plant Pathol* 49 (2), 77–79 (3p (Persian Language)).
- Mirabolfothy, M., Groenewald, J.Z., Crous, P.W., 2011. The occurrence of charcoal disease caused by *Biscogniauxia mediterranea* on chestnut-leaved oak (*Quercus castaneifolia*) in the Golestan Forests of Iran. *Plant Dis.* 95, 876. <https://doi.org/10.1094/PDIS-03-11-0153>.
- Naimi, B., 2017. RTS: Raster Time Series Analysis. Available online. <https://cran.r-project.org/web/packages/rts/index.html> (accessed on 20.12.2018).
- Nowak, D.J., Greenfield, E.J., 2010. Evaluating the National Land Cover Database tree canopy and impervious cover estimates across the conterminous United States: a comparison with photo-interpreted estimates. *Environ. Manag.* 46 (3), 378–390. <https://doi.org/10.1007/s00267-010-9536-9>.
- O'Halloran, T.L., Law, B.E., Goulden, M.L., Wang, Z., Barr, J.G., Schaaf, C., Brown, M., Fuentes, J.D., Göckede, M., Black, A., Engel, V., 2012. Radiative forcing of natural forest disturbances. *Glob. Chang. Biol.* 18, 555–565. <https://doi.org/10.1111/j.1365-2486.2011.02577.x>.
- Olfat, A.M., Pourtahmasi, K., 2010. Anatomical characters in three oak species (*Q. libani*, *Q. brantii* and *Q. infectoria*) from Iranian Zagros Mountains. *Aust. J. Basic Appl. Sci.* 4, 3230–3237.
- Pitman, A.J., De Noblet-Ducoudré, N., Cruz, F.T., Davin, E.L., Bonan, G.B., Brovkin, V., Claussen, M., Delire, C., Ganzeveld, L., Gayler, V., Van Den Hurk, B.J.J.M., Lawrence, P.J., Van Der Molen, M.K., Müller, C., Reick, C.H., Seneviratne, S.I., Strengren, B.J., Voldoire, A., 2009. Uncertainties in climate responses to past land cover change: first results from the LUCID intercomparison study. *Geophys. Res. Lett.* 36. <https://doi.org/10.1029/2009GL039076>.
- Pourreza, M., Hosseini, S.M., Sinegani, A.A.S., Matiniazadeh, M., Dick, W.A., 2014. Soil microbial activity in response to fire severity in Zagros oak (*Quercus brantii*

- Lindl.) forests, Iran, after one year. *Geoderma* 213, 95–102. <https://doi.org/10.1016/j.geoderma.2013.07.024>.
- Román, M.O., Schaaf, C.B., Woodcock, C.E., Strahler, A.H., Yang, X., Braswell, R.H., Curtis, P.S., Davis, K.J., Dragoni, D., Goulden, M.L., Gu, L., Hollinger, D.Y., Kolb, T.E., Meyers, T.P., Munger, J.W., Privette, J.L., Richardson, A.D., Wilson, T.B., Wofsy, S.C., 2009. The MODIS (Collection V005) BRDF/albedo product: Assessment of spatial representativeness over forested landscapes. *Remote Sens. Environ.* 113, 2476–2498. <https://doi.org/10.1016/j.rse.2009.07.009>.
- Running, S.W., 2008. Climate change: ecosystem disturbance, carbon, and climate. *Science* 321, 652–653. <https://doi.org/10.1126/science.1159607> (80-).
- Sadeghi, M., Malekian, M., Khodakarami, L., 2017. Forest losses and gains in Kurdistan province, western Iran: where do we stand? *Egypt. J. Remote Sens. Sp. Sci.* 20, 51–59. <https://doi.org/10.1016/j.ejrs.2016.07.001>.
- Safaei, D., Khodaparast, S.A., Mirabolfathy, M., Mousanejad, S., 2016. Relationship between dieback of Persian oak (*Quercus brantii*) and apparent and latent infection of *Biscogniauxia mediterranea* in Zagros forests. *Iran J. Plant Pathol.* 52 (ISSN: 0006-2774).
- Schwaiger, H.P., Bird, D.N., 2010. Integration of albedo effects caused by land use change into the climate balance: should we still account in greenhouse gas units? *For. Ecol. Manag.* 260, 278–286. <https://doi.org/10.1016/j.foreco.2009.12.002>.
- Smith, M.J., Palmer, P.L., Purves, D.W., Vanderwel, M.C., Lyutsarev, V., Calderhead, B., Joppa, L.N., Bishop, C.M., Emmott, S., 2014. Changing how earth system modeling is done to provide more useful information for decision making, science, and society. *Bull. Am. Meteorol. Soc.* 95, 1453–1464. <https://doi.org/10.1175/BAMS-D-13-00080.1>.
- STP, 2015. GIS Layer of Soil Type in Iran. URL <http://girs.ir/%D9%84%D8%A7%DB%8C%D9%87-%D8%AE%D8%> (Accessed: 20.12.2018).
- Taghimollaei, Y., Karamshahi, A., 2017. Sudden oak death in Iran forests. *International Journal of Forest, Soil & Erosion* 7 (1).
- Team, R., 2018. R: A Language and Environment for Statistical Computing.
- Trigo, R.M., Gouveia, C.M., Barriopedro, D., 2010. The intense 2007–2009 drought in the Fertile Crescent: impacts and associated atmospheric circulation. *Agric. For. Meteorol.* 150, 1245–1257. <https://doi.org/10.1016/j.agrformet.2010.05.006>.
- Van der Werf, G.R., Randerson, J.T., Giglio, L., van Leeuwen, T.T., Chen, Y., Rogers, B.M., Mu, M., van Marle, M.J.E., Morton, D.C., Collatz, G.J., Yokelson, R.J., Kasibhatla, P.S., 2017. Global fire emissions estimates during 1997–2015. *Earth Syst. Sci. Data Discuss.* 9, 1–43. <https://doi.org/10.5194/essd-2016-62>.
- Vannini, A., Lucero, G., Anselmi, N., Vettriano, A.M., 2009. Response of endophytic *Biscogniauxia mediterranea* to variation in leaf water potential of *Quercus cerris*. *For. Pathol.* 39, 8–14. <https://doi.org/10.1111/j.1439-0329.2008.00554.x>.
- Veraverbeke, S., Lhermitte, S., Verstraeten, W.W., Goossens, R., 2010b. The temporal dimension of differenced Normalized Burn Ratio (dNBR) fire/burn severity studies: the case of the large 2007 Peloponnese wildfires in Greece. *Remote Sens. Environ.* 114, 2548–2563. <https://doi.org/10.1016/j.rse.2010.05.029>.
- Veraverbeke, S., Van De Kerchove, R., Verstraeten, W., Lhermitte, S., Goossens, R., 2010a. Fire-induced changes in vegetation, albedo and land surface temperature assessed with MODIS. 30th EARSeL symposium: Remote Sensing for Science, Education, and Natural and Cultural Heritage. European Association of Remote Sensing Laboratories (EARSeL), pp. 431–438. URL <https://biblio.ugent.be/publication/1087213/file/1087537.pdf> (Accessed: 20.12.2018).
- Verbesselt, J., Hyndman, R., 2010. Detecting trend and seasonal changes in satellite image time series. *Remote Sens. Environ.* 114, 106–115. <https://doi.org/10.1016/j.rse.2009.08.014>.
- Verbyla, D.L., Kasischke, E.S., Hoy, E.E., 2008. Seasonal and topographic effects on estimating fire severity from Landsat TM/ETM+ data. *Int. J. Wildland Fire* 17, 527–534. <https://doi.org/10.1071/WF08038>.
- Voss, K.A., Famiglietti, J.S., Lo, M., De Linage, C., Rodell, M., Swenson, S.C., 2013. Groundwater depletion in the Middle East from GRACE with implications for transboundary water management in the Tigris-Euphrates-Western Iran region. *Water Resour. Res.* 49, 904–914. <https://doi.org/10.1002/wrcr.20078>.